DOI 10.4430/bgta0230

Examining the crustal structures of eastern Anatolia, using thermal gradient, heat flow, radiogenic heat production and seismic velocities (V_p and V_s) derived from Curie Point depth

A. Cirmik

Department of Geophysical Engineering, Dokuz Eylul University, İzmir, Turkey

(Received: 14 February 2018; accepted: 24 April 2018)

ABSTRACT Eastern Anatolia is one of the most active volcanic and tectonic systems, caused by the covergence of Arabian and Anatolian Plates. In this study, the crustal and thermal structures of eastern Anatolia are investigated by using the values derived from Curie Point depth (CPD). The thermal gradient, the radiogenic heat production and seismic compressional velocity (V_p) values of eastern Anatolia are obtained using calculated CPD. Additionally, seismic shear velocities (V_s) of eastern Anatolia are calculated by CPD values for the first time in this study. The calculated V_s values prove consistent with the V_s values obtained by a previous seismic study. Therefore, it can be said that V_s values can be obtained for an area that includes the aeromagnetic data in the case of absence of seismic studies. Finally, the heat flow and V_s values are evaluated with the focal depth distribution of the earthquakes to investigate the crustal features. The existence of high heat flow, high seismicity and low V_s values along the eastern Anatolian Fault Zone and around Karliova Triple Junction indicate that these regions have high geothermal potential.

Key words: eastern Anatolia, thermal gradient, heat flow, heat production, S-wave velocity.

1. Introduction

In the Alpine-Himalayan Belt, one of the youngest continent-continent collision occurres between the Arabian and Anatolian Plates (Fig. 1a). Eastern Anatolia has a complex tectonic mechanism and a high topography with a ~2 km high elevated plateau and Neogene and Holocene volcanics as the result of the collision. As a result of the compressional tectonic regime, the Anatolian Plate was cut by the right-lateral North Anatolian Fault Zone (NAFZ) and the left-lateral East Anatolian Fault Zone (EAFZ) (McKenzie, 1972; Burke and Şengör, 1986; Bozkurt, 2001). Additionally, this region is dominated by the Bitlis Zagros Suture Zone (BZSZ) (Koçyiğit *et al*., 2001) (Figs. 1 and 2).

Eastern Anatolia has active faults and volcanic activity (Fig. 2), therefore, it is very significant to investigate the tectonism and subsurface features of the region for receiving information about the brittle-ductile transition of the crust, crustal thickness, lithospheric and asthenospheric boundary. Due to the complex tectonic structure of the eastern region, numerous

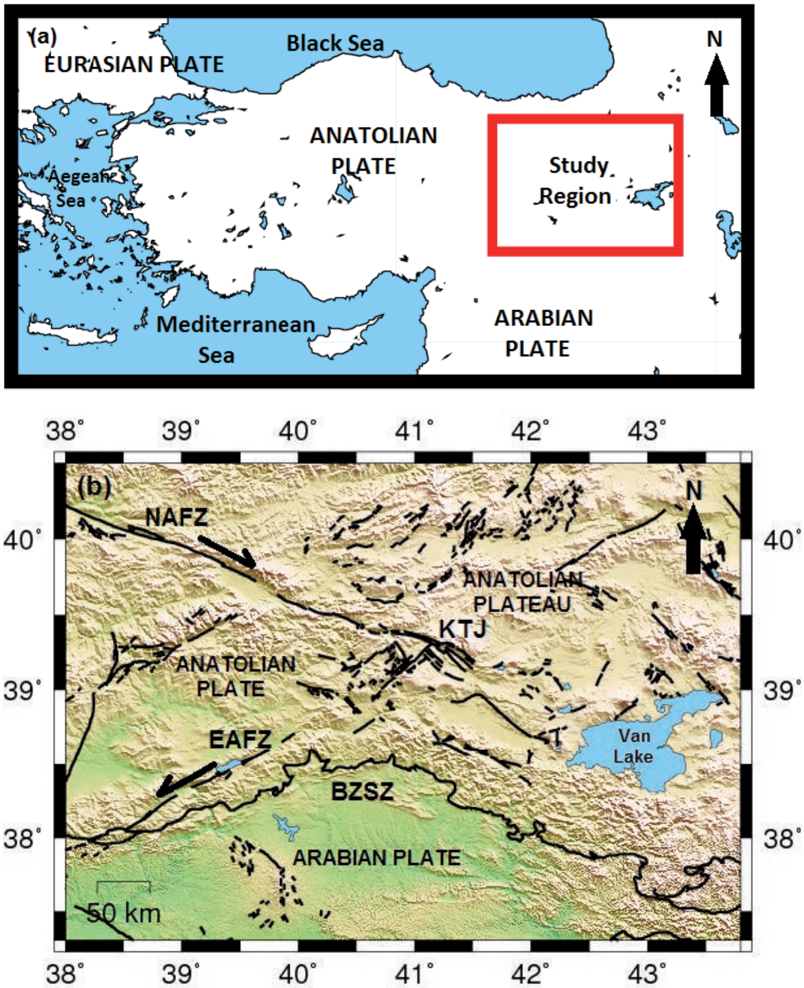

Fig. 1 - Simplified map of Turkey (Anatolia): a) the red rectangle shows the location of the study area, eastern Anatolia; b) regional tectonic map of the study region (eastern Anatolia) with topographic relief. Legenda: EAFZ = East Anatolia Fault Zone, NAFZ = North Anatolia Fault Zone; BZSZ = Bitlis Zagros Suture Zone, KTJ = Karliova Triple Junction (modified from Bozkurt, 2001).

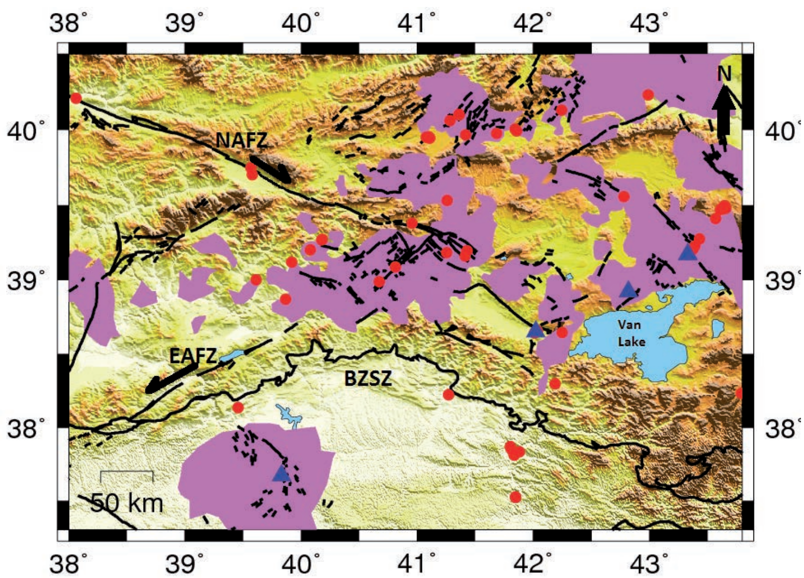

Fig. 2 - Regional tectonic map of eastern Anatolia (study region) with topographic relief (EAFZ: East Anatolia Fault Zone, NAFZ: North Anatolia Fault Zone; BZSZ: Bitlis Zagros Suture Zone, modified from Bozkurt, 2001), Neogene volcanic regions (lilac areas), Holocene volcanoes (blue triangles) (Zor *et al*., 2003), and hot spots (red circles) (MTA, 2005).

studies (McKenzie, 1972; Rotstein and Kafka, 1982; Dewey *et al*., 1986; Pearce *et al*., 1990; Al-Lazki *et al*., 2003; Gök *et al*., 2003, 2007; Keskin, 2003; Sandvol *et al*., 2003; Şengör *et al*., 2003; Türkelli *et al*., 2003; Zor *et al*., 2003; Gürbüz *et al*., 2004; Bektaş *et al*., 2007; Pamukçu *et al*., 2007, 2014, 2015; Özaçar *et al*., 2008; Pamukçu and Akçığ, 2011; Bektaş, 2013; Oruç *et al*., 2017) have been undertaken in the region to investigate the geodynamic models, lithospheric-asthenospheric features and the thermal structures of eastern Anatolia.

According to Şengör *et al*. (2003), in the Anatolian Plateau with the addition of the mantle to the topography, the crustal thickness is thin and the mantle lid is non-existent. In the Gök *et al*. (2007) study, based on V_s calculations with receiver function analysis, very low upper mantle velocities were calculated to the east of the Karliova Triple Junction (KTJ) (surrounding the Anatolian Plateau, Fig. 1b). In this area the asthenospheric materials took place of lithospheric mantle.

According to Pamukçu *et al*. (2007), the crustal thickness of eastern Anatolia, which was obtained by applying the moving windows power spectrum analysis to the gravity data, increases from 38 to 52 km from the south to the north. In the studies of Zor *et al*. (2003) and Gürbüz *et al*. (2004), the mean crustal thickness of eastern Anatolia was found to be 45 km. The crustal thickness, which is 42 km to the south of BZSZ, extends to 50 km throughout NAFZ and increases from 40 to 46-48 km north of the Arabian Plate to the centre of the Anatolian Plateau (Zor *et al*., 2003; Gürbüz *et al*., 2004). In the study of Türkelli *et al*. (2003), due to the lack of lithospheric mantle in some areas of eastern Anatolia, very low Pn velocities (lower than 7.8 km/s) were obtained particularly east of the Anatolian Plateau and the Anatolian Plate. Gök *et al*. (2007) pointed out that the lack of subcrustal earthquakes in the Arabian Plate and the Anatolian Plateau was related to the non-existence of the Arabian Plate subduction under the Anatolian Plateau.

The Curie Point depth (CPD) estimates the average depth of magnetic sources and is considered to reflect thermal structures and volcanic fields. CPD analysis allows determining the depth at which the magnetite passes from a ferromagnetic to paramagnetic state and there is a relationship between the thicknesses of the crust. CPD investigations including information about the crustal features have been used in various studies (e.g. Bhattacharrya and Morley, 1965; Okubo *et al*., 1985; Tsokas *et al*., 1998; Tanaka *et al*., 1999; Ateş *et al*., 2005; Aydın *et al*., 2005; Dolmaz *et al*., 2005; Bektaş *et al*., 2007; Bilim, 2007; Saleh *et al*., 2013; Obande *et al*., 2014; Pamukçu *et al*., 2014; Bilim *et al*., 2016). Therefore, the regions characterized by shallower CPD values are related to the thinner crust and high geothermal potential (Pamukçu *et al*., 2014).

In the light of this knowledge, eastern Anatolia, a very complex region, was examined by using thermal gradient, heat flow, heat production and seismic values obtained from CPD values and compared with previous studies. In this study, the CPD values of eastern Anatolia, which were obtained by Pamukçu *et al*. (2014) from the aeromagnetic data [the Directorate of Mineral Research and Exploration of Turkey (MTA, 2005) in the scope of N.101Y124, The Scientific and Technological Research Council of Turkey (TUBITAK) project] using spectrum analysis of Okubo *et al*. (1985), were initially used for calculating the thermal gradient, the heat flow and the heat production values of eastern Anatolia. Additionally, P-wave (V_p) and S-wave (V_s) velocities of eastern Anatolia were calculated using the empiric relation between the heat production and the seismic velocities. Finally, the resulting values were evaluated together with the previous studies and focal depth distributions of earthquakes.

As a first step in the study, the thermal gradient values of eastern Anatolia were calculated, with values varying between 20 ºC/km and 100 ºC/km. Then, the heat flow values which indicate the thermal characteristics of the crust were estimated for different thermal conductivity values (k = 2.5 $Wm^{-1}K^{-1}$ and k = 2.7 $Wm^{-1}K^{-1}$), the values varying between 50 and 250 and 50 and 265 mW/m^2, respectively. As a third step, the heat production values were calculated for different near-surface radiogenic heat production rate coefficients (A_0 = 1.5 μWm^{-3}, A_0 = 3 μWm^{-3} and A_0 = 4 μWm^{-3}); the heat production values range between 0.10-0.85 $\mu W/m^3$, 0.2-1.6 $\mu W/m^3$ and 0.2-2.3 $\mu W/m^3$. Finally, V_p were estimated for each heat production values, which were obtained by different A_0 values and vary between 5.9-6.9 km/s (for heat production value estimated by A_0 = 1.5 μWm^{-3}), 5.6-6.6 km/s (for heat production value estimated by A_0 = 3 μWm^{-3}) and 5.45-6.45 km/s (for heat production value estimated by A_0 = 4 μWm^{-3}). Additionally, V_s were calculated for the first time in this study for each V_p value by using the relation between seismic velocities. These vary between 3.42-3.96 km/s (for V_p estimated by A_0 = 1.5 μWm^{-3}), 3.22-3.76 km/s (for V_p estimated by A_0 = 3 μWm^{-3}) and 3.14-3.68 km/s (for V_p estimated by A_0 = 4 μWm^{-3}). The V_s values obtained indirectly from heat production values estimated for A_0 = 3 μWm^{-3}, are found to be consistent with the V_s values of Zor *et al.* (2003), which were obtained by receiver function. Therefore, it is safe to say that V_s values can be estimated for a region by using CPD values obtained from aeromagnetic data.

Finally, the focal depth distributions of earthquakes (M≥2.5), occurring between 1973 and 2016 up to 50 km depth in the region, were evaluated together with the heat flow and V_s values, therefore the crustal features of eastern Anatolia are investigated.

2. Methodology and estimations of thermal features of eastern Anatolia

2.1. Determination of CPD

CPD is a significant value to determine the magnetic bottom of the crust, since the crustal minerals which represent ferromagnetic features lose their magnetism and change to paramagnetic features related to the temperature increase at this depth. Regions with shallow CPD values are related to the thin crust and geothermal and volcanic structures (Pamukçu *et al.*, 2014). CPD values used for determining the thermal structure of the crust (Okubo *et al.*, 1985; Ateş *et al.*, 2005; Bilim, 2007, 2011; Saleh *et al.*, 2013; Obande *et al.*, 2014; Pamukçu *et al.*, 2014; Bilim *et al.*, 2016), are estimated from aeromagnetic anomaly data using the magnetic spectral method (Spector and Grant, 1970; Okubo *et al.*, 1985). A relationship between the power spectrum of magnetic anomalies and the depth of the magnetic sources is presented and the data is transformed into frequency domain with this method. In this method, the Curie depths (z_b) are calculated by using the equation:

$$z_b = 2z_0 - z_t \tag{1}$$

where z_t is the depth of the top of the magnetic source and z_0 the depth of the centre of the magnetic source.

2.2. Determination of the thermal gradient, the heat-flow and the radiogenic heat production

Thermal gradient (*grad T, ∂T/∂z*) values are obtained by dividing the Curie temperature (580 ºC) value to the CPD values:

$$grad\ T = \frac{-580°\ C}{CPD\ (z_b)}\ . \tag{2}$$

There is an inverse relationship between the heat flow values and CPD values. In other words, if the heat flow values are high in a region, this region has shallow CPD values; conversely, if the heat flow values are low, the region is related to deep CPD values (Pamukçu *et al*., 2014; Bilim *et al*., 2016). The heat flow (q_0) values are estimated (Turcotte and Schubert, 1982; Artemieva and Money, 2001) by:

$$q_0 = grad\ T * k \tag{3}$$

where k is the thermal conductivity.

Ever since the universe has existed, natural radioactivity has continued up to the present due to the long half-lives of numerous radioactive element series. By using radiometric methods, the geochemical and geological mapping and radiogenic heat production calculations can be accomplished. A great amount of the source of the crustal radiogenic heat production is the decay of the heat producing elements, namely Uranium^{-238} (238U), Uranium^{-235} (235U), Thorium^{-232} (232Th), and Potassium^{-40} (40K) (Durrance, 1986; Uyanık and Akkurt, 2010; Uyanik *et al*., 2010, 2015). Lachenbruch (1970) devised an exponential decay model that provides the radiogenic heat production of the continental crust dependent on depth. Therefore, the heat production (A) is calculated as the function of depth [$A(z)$] by:

$$A(z) = A_0 \exp\left(\frac{-z}{D}\right) \tag{4}$$

where A_0 is the radiogenic heat production rate coefficient measured in near-surface rocks, z is CPD values, and D is the radiogenic scaling depth representing the characteristic depth over the heat producing elements (Lachenbruch, 1968; Artemieva and Money, 2001).

2.3. Estimation of V_p and V_s from the heat production

There is an empirical relationship between the P-wave seismic velocity (V_p, km/s) and heat production (A, Wm^{-3}) (Rybach, 1978/1979; Rybach and Buntebarth, 1982, 1984; Correia and Ramalho, 1999), which is given as:

$$\ln A = 12.6 - 2.17\ V_p\ . \tag{5}$$

By this equation, the V_p values presenting the significant case for clarifying the brittle-ductile transition of the crust are estimated. There is an inverse relationship between the V_p values and the heat production (A); in a region containing crystalline elements, while V_p values increase, inversely the heat production values decrease (Rybach, 1978/1979).

By obtaining the V_p values of a region, V_s values can be estimated by using the well-known relation between the velocities:

$$\frac{V_p}{V_s} = \left[2 \cdot \frac{(1-\mu)}{(1-2\cdot\mu)}\right]^{\frac{1}{2}} \tag{6}$$

where μ is the Poisson ratio and it is assumed as 0.25 for the crust (Christensen, 1996).

3. Applications

In this study, CPD values (Fig. 3) obtained by applying the spectrum analysis of Okubo *et al*. (1985) on aeromagnetic data by Pamukçu *et al*. (2014), were used. In the study of Pamukçu *et al*. (2014), the aeromagnetic data were surveyed by MTA (2005) in eastern Anatolia between 37º-44º E and 37º-42º N with 1 km sampling intervals, and were reduced to the north magnetic pole. The data were separated into 154 overlapping blocks with dimensions 90×90 km^2, the averaged log power spectrum was calculated for each divided block, and the depths (z_b, z_0, z_t) were measured by using Eq. 1 for each block.

Firstly, the thermal gradient values of the region (Fig. 4) were calculated using Eq. 2, where the Curie temperature of the domain is assumed as 580 ºC (Okubo *et al*., 1985). As a second step, the heat flow values of the study area were calculated by using Eq. 3 with these thermal gradient values and for different thermal conductivity (k) values. In the studies of Springer (1999) and Artemieva and Money (2001), it was suggested that thermal conductivity (k) varies between 2.5 and 3.0 Wm^{-1}K^{-1} for the upper crust. In this study, the heat flow values are estimated by assuming k as 2.5 and 2.7 Wm^{-1}K^{-1} (Fig. 5). As a third step, the heat production (A) values were obtained (Fig. 6), by assuming the coefficient D as 10 km (Lachenbruch, 1968; Jaupart, 1986) and near-surface radiogenic heat production rate coefficients (A_0) as 1.5 µWm^{-3}, 3 µWm^{-3} and 4 µWm^{-3} (Springer, 1999) with Eq. 4.

As the last step, the V_p values of eastern Anatolia are estimated for the heat production values obtained with A_0=1.5 µWm^{-3}, A_0=3 µWm^{-3} and A_0= 4 µWm^{-3} by using Eq. 5 (Fig. 7) and finally, V_s values are calculated with the aid of Eq. 6 for each V_p value (Fig. 8).

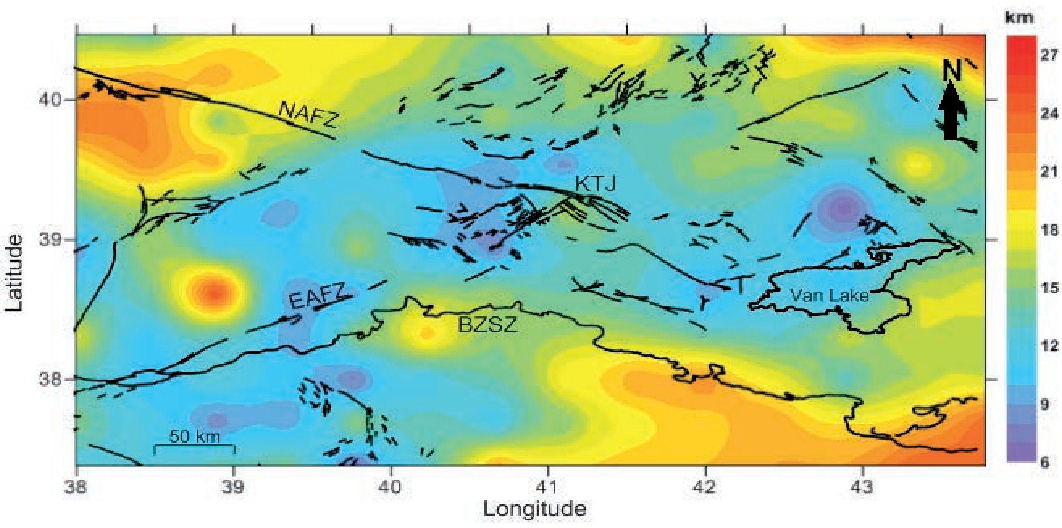

Fig. 3 - CPD values of eastern Anatolia.

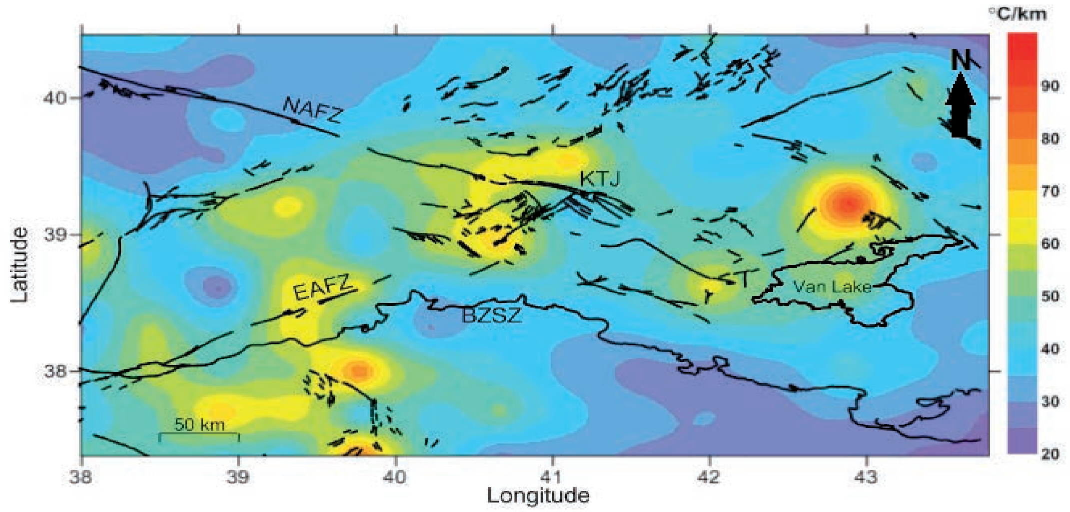

Fig. 4 - The thermal gradient values of eastern Anatolia.

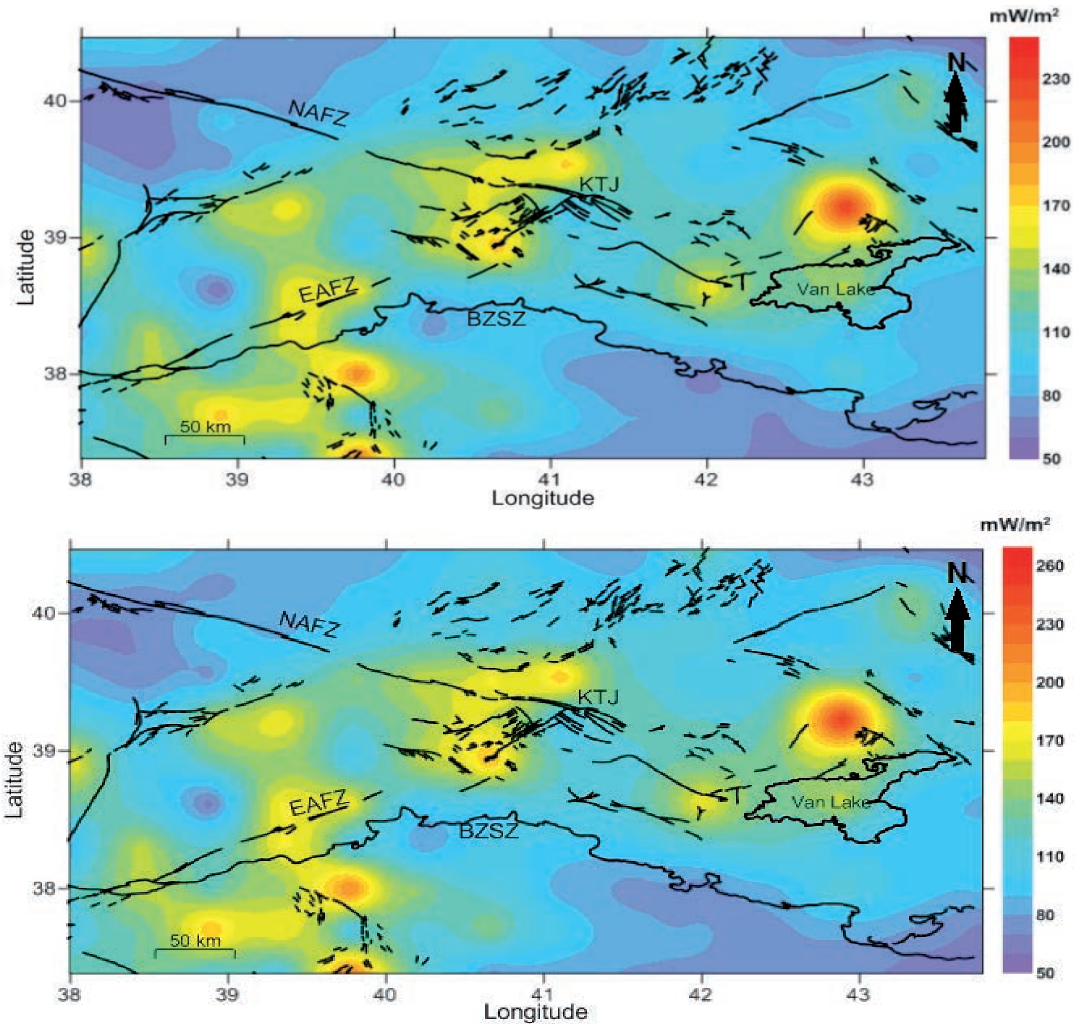

Fig. 5 - The heat flow values of eastern Anatolia which are estimated by using thermal conductivity (k) as 2.5 W m^{-1}K^{-1} (a) and as 2.7 W m^{-1}K^{-1} (b).

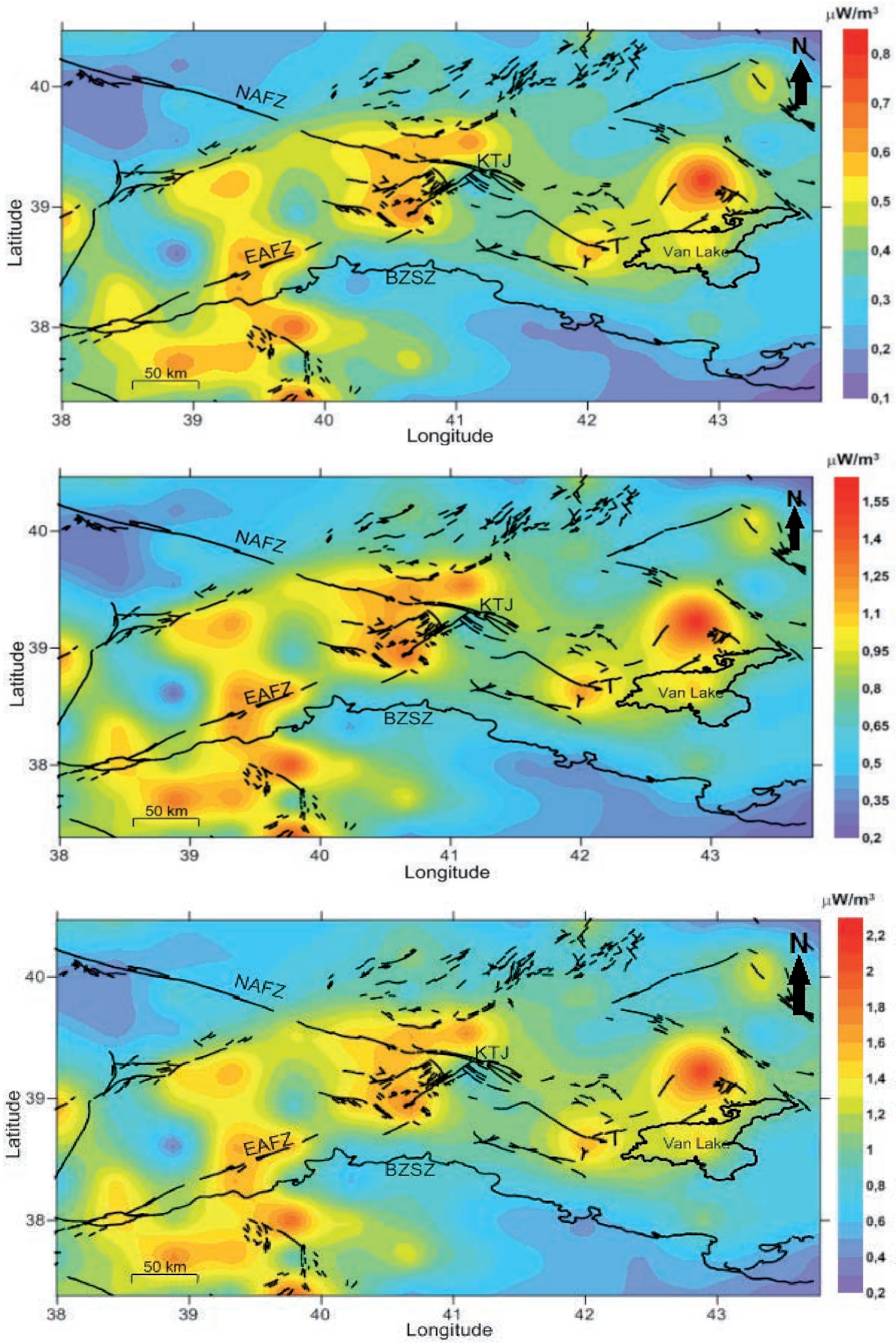

Fig. 6 - The heat production values of eastern Anatolia which are estimated by using near-surface radiogenic heat production rate coefficient (A_0) as 1.5 µWm^{-3} (a), 3 µWm^{-3} (b), and 4 µWm^{-3} (c).

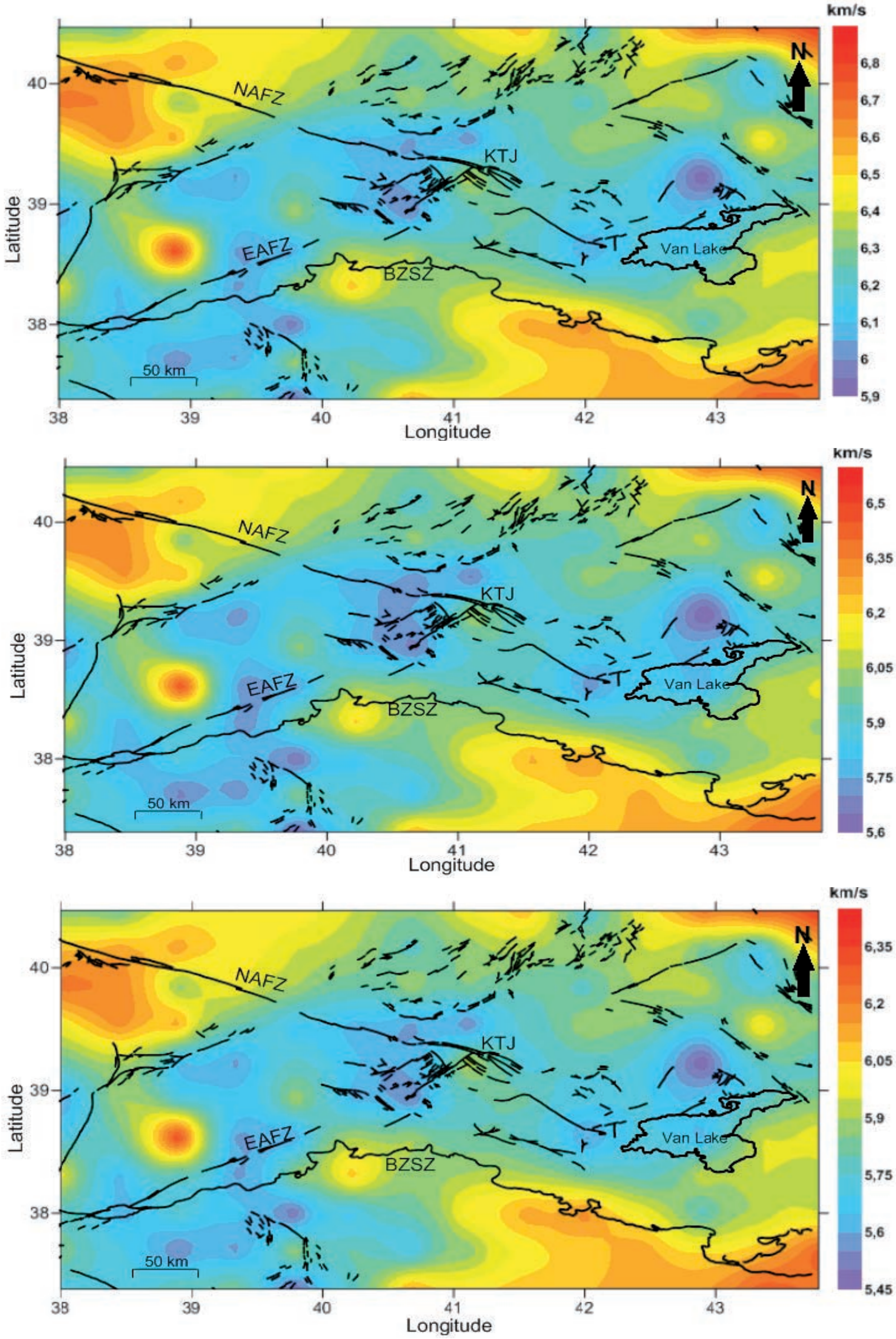

Fig. 7 - V_p of eastern Anatolia which are estimated from the heat production values obtained by using A_0 as 1.5 μWm^{-3} (a), 3 μWm^{-3} (b), and 4 μWm^{-3} (c).

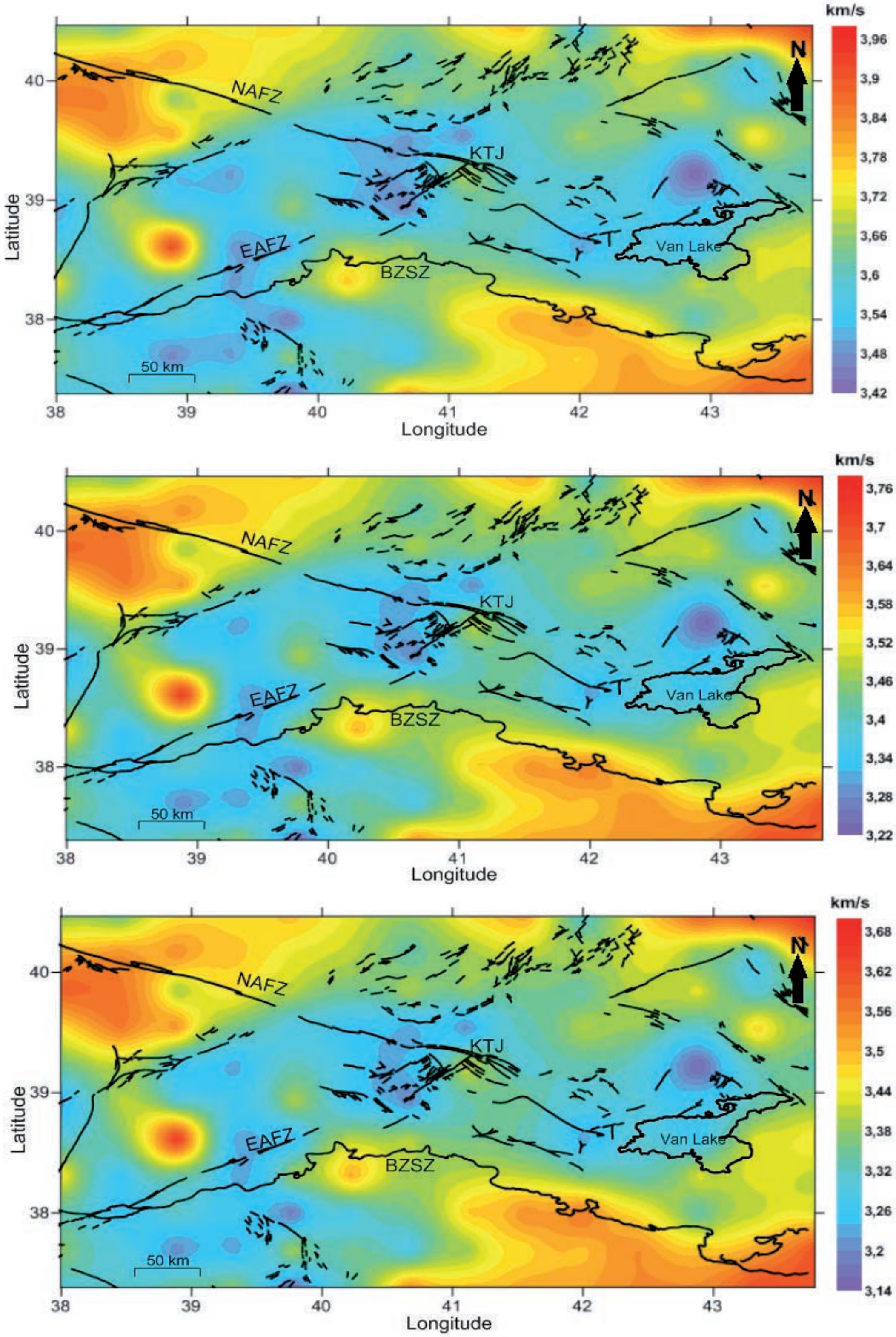

Fig. 8 - V_s of eastern Anatolia which are estimated from V_p values obtained by using A_0 as 1.5 μWm^{-3} (a), 3 μWm^{-3} (b), and 4 μWm^{-3} (c).

4. Results and discussions

In this study, the thermal gradient, the heat flow, the heat production, and V_p and V_s values of eastern Anatolia, were calculated using CPD values in order to examine the crustal features of eastern Anatolia. In Fig. 3, the CPD values obtained by Pamukçu *et al*. (2014) range between 6 and 27 km. The shallower CPD values (Fig. 3) are generally seen in the regions where the Holocene and Neogene volcanic and hot spots are located (Fig. 2). In other words, CPDs are shallower around Lake Van and to the SW of BZSZ, south of the Anatolian Plateau and in the region where NAFZ and EAFZ meet (Fig. 3) relative to other parts of the eastern Anatolia region.

In the next step of this study, the thermal gradient and heat flow distributions of the study area were investigated. The thermal gradient values are found to be between 20 and 100 ºC/km. Then, the heat flow values which indicate the thermal characteristics of the crust were estimated for different thermal conductivity values ($k = 2.5$ $Wm^{-1}K^{-1}$ and $k = 2.7$ $Wm^{-1}K^{-1}$), with values varying between 50-250 mW/m^2 and 50-265 mW/m^2, respectively (Fig. 5). In this study, the higher heat flow values are found in the regions where the shallower CPD values are determined (Figs. 3 and 5), the highest heat flow values being obtained in the northern part of Lake Van (Fig. 5). Additionally, the CPD values are shallower than the Moho depth; therefore, Pamukçu *et al*. (2014) suggested that the magnetic sources in the study area were located in the upper crust.

The study of Pollack and Chapman (1977) highlighted that the heat flow values change in relation to the age of the tectonic movements and that the heat flow values are higher in the younger tectonic regions. According to the study of Keskin (2003), based on radiogenic dating, the volcanic activity began earlier in the north compared to the south and the age of the volcanic activity is found to be younger from the latitude 40º toward 38º, i.e. 11 Myr at latitude 40º and 2 Myr at latitude 38.5º. When this knowledge is evaluated together with the CPD, thermal gradient and heat flow maps (Figs. 3, 4 and 5), the regions having shallower CPD and high thermal gradient and heat flow values represent volcanic features (Fig. 2). The heat flow values obtained in this study are coherent with this knowledge and the results of tectonic age investigations by Keskin (2003).

According to the study by Zor *et al*. (2003), based on the features of the volcanic products, the origin of the heat sources differs for each of the regions where the heat production and heat flow values are high, namely surrounding EAFZ (Fig. 1). According to Keskin (2003), the Holocene volcanoes surrounding Lake Van play an important role in the variation of the lava chemistry.

The heat production values are calculated for different near-surface radiogenic heat production rate coefficients as $A_0 = 1.5$ μWm^{-3}, $A_0 = 3$ μWm^{-3} and $A_0 = 4$ μWm^{-3} (Fig. 6). The heat production values calculated with $A_0 = 1.5$ μWm^{-3}, $A_0 = 3$ μWm^{-3} and $A_0 = 4$ μWm^{-3} vary between 0.10-0.85 $\mu W/m^3$ (Fig. 6a), 0.20-1.60 $\mu W/m^3$ (Fig. 6b) and 0.20-2.30 $\mu W/m^3$ (Fig. 6c), respectively. In the last step, V_p are estimated for each heat production value obtained by different A_0 values and vary between 5.9-6.9 km/s (for heat production value estimated by $A_0 = 1.5$ μWm^{-3}; Fig. 7a), 5.60-6.60 km/s (for $A_0 = 3$ μWm^{-3}; Fig. 7b) and 5.45-6.45 km/s (for $A_0 = 4$ μWm^{-3}; Fig. 7c). In this study, the S-wave velocities (V_s) are calculated for eastern Anatolia for the first time using aeromagnetic data. Here, V_s values are estimated for each V_p value by using the relation between seismic velocities (Eq. 6) and are found to vary between 3.42-3.96 km/s (for V_p estimated by $A_0 = 1.5$ μWm^{-3}; Fig. 8a), 3.22-3.76 km/s (for V_p estimated by $A_0 = 3$ μWm^{-3}; Fig. 8b) and 3.14-3.68 km/s (for V_p estimated by $A_0 = 4$ μWm^{-3}; Fig. 8c). The V_s values, which were obtained indirectly from heat production values estimated for $A_0 = 3$ μWm^{-3} in this study, are found to be consistent with the mean V_s distributions of Zor *et al*.

(2003), which were obtained from seismological data, finding on average a 45 km crustal thickness. This result, obtained for the first time in the literature for eastern Anatolia, is the most significant finding of this study. Therefore, it is clear that the seismic velocity distribution interpretations can be realized with the aid of V_s values obtained by CPD values of the region.

Under ideal geophysical conditions, in the crust V_p and V_s are generally 6.5 and 2.5 km/s, respectively. These velocities rise to 8.1 and 3.4 km/s, respectively, in the upper mantle boundary at 100 km depth. In this study, V_p values vary between 5.45-6.90 km/s, the minimum velocity is estimated for $A_0 = 4$ μWm^{-3} (Fig. 7c) and the maximum velocity is estimated for $A_0 = 1.5$ μWm^{-3} (Fig. 7a). V_s values vary between 3.14-3.96 km/s related with the V_p values. The minimum and the maximum velocities are reported in Figs. 8a and 8c, respectively. Therefore, the estimated velocities in this study are in accordance with the geophysical conditions.

Sandvol *et al*. (2003) indicated the directions of the upper mantle/asthenospheric flows for eastern Anatolia (Fig. 9) in their study. In the region where the directions of the mantle flows are crossing each other (Fig. 9), the CPD values are shallow (Fig. 3), the heat production values (Fig. 6) are high, therefore, the seismic velocities (V_p and V_s) are slow (Fig. 7 and 8). If the mantle flows (Fig. 9) located in southern BZSZ are investigated, the absence of the mantle flow towards SE is coherent with the relatively deeper CPD values and lower thermal gradient and heat production values (Figs. 3, 4, 6). The mantle flow investigations of Sandvol *et al*. (2003), are consistent with the regional extending of volcanoes and hotspot areas (Fig. 2), shallow CPD (Fig. 3), high heat flow (Fig. 5) and heat production values (Fig. 6) and slow V_p (Fig. 7) and V_s (Fig. 8) values which are obtained in this study.

The existence of earthquakes and focal depth distributions represent a significant knowledge on the lithospheric features such as brittle-ductile transition zones. Therefore, the focal depth distributions of earthquakes ($M \geq 2.5$) occurring between 1973 and 2016 [obtained from United States Geological Survey (USGS)], are examined initially with heat flow to investigate the brittle-ductile transition zone and the relationship with the thermal features of eastern Anatolia in Fig. 10. It can be seen that the earthquakes generally occurred in the regions having low heat flow values (Fig. 10). According to Watts (2001) and Pamukçu *et al*. (2014), in the regions with high seismicity and low heat flow values, the elastic zone is thick. Therefore, it may be inferred that the regions (west side of NAFZ, the region located to the NE of KTJ, eastern side of BZSZ and eastern side of Lake Van) seen in Fig. 10 with high seismic activity and low heat values, can be related to the existence of the thick elastic zone. In particular, the surrounding area of EAFZ includes magma-crust intersection (Zor *et al*., 2003) and the reason for high seismicity is the rigid crust made up of a highly brittle partion and plumb-like magma. Additionally, in the regions shown by dashed squares in Fig 10, the absence of earthquakes is notable and these regions show high heat flow values. The absence of seismicity is, therefore, related to the low crustal rigidity and the crust is dominated by a ductile part (Fig. 10). To further investigate the crustal features of the study region in detail and evaluate the earthquakes with seismic velocities, the focal depth distributions are drawn from the surface to 50 km depth on the V_s maps (Fig. 11). If all focal depth distributions are investigated, it can be observed that the greatest number of earthquakes occurred from the surface down to 10 km depth (Fig. 11a) and from 10 to 20 km depth (Fig. 11b). It can be deduced that the brittle part of eastern Anatolia is approximately down to 20 km depth and the rigid part of the crust is between 10 and 20 km depths. This result is consistent with the effective elastic thickness of eastern Anatolia which was found to be 15 km

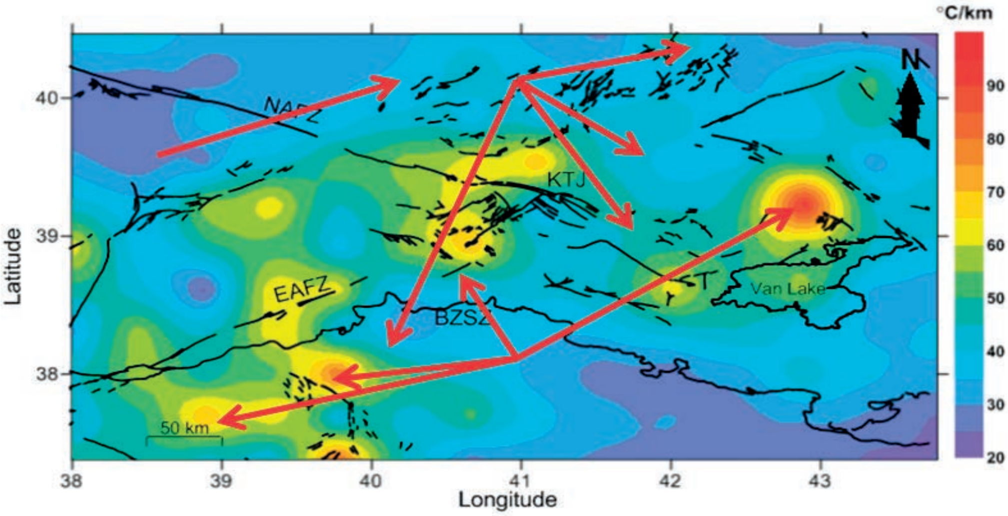

Fig. 9 - Thermal gradient values of eastern Anatolia. The red vectors represent the directions of possible asthenospheric flows according to Sandvol *et al.* (2003).

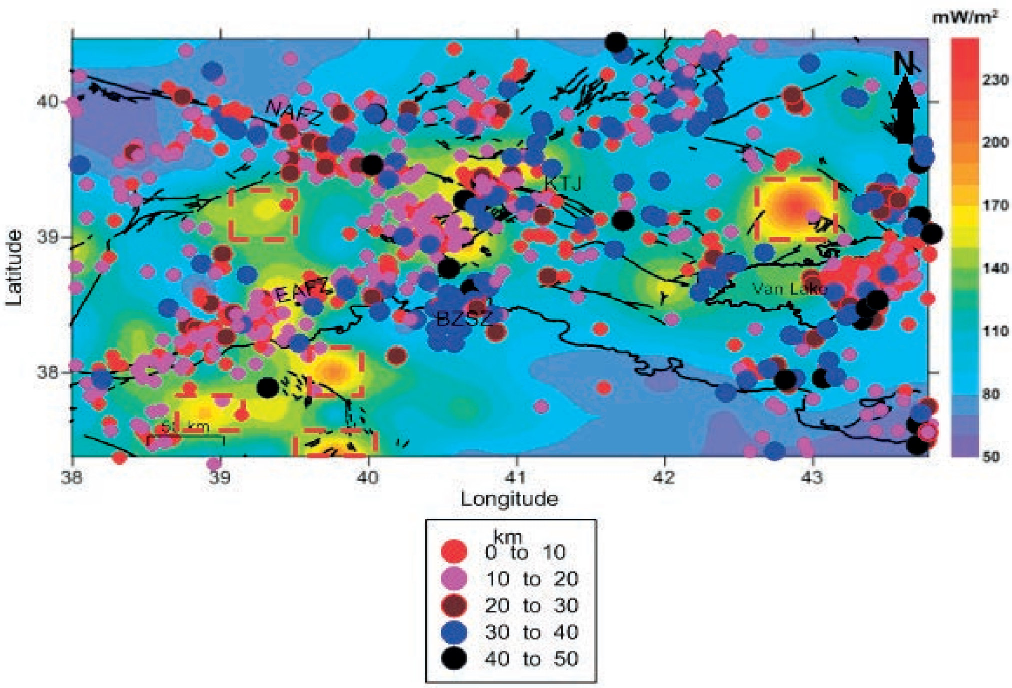

Fig. 10 - Focal depth distributions of earthquakes ($M \geq 2.5$) occurred between 1973 and 2016 (https://earthquake.usgs.gov/earthquakes/search/) on the heat flow map obtained by using k as 2.5 W m^{-1}K^{-1}. Red dashed squares represent non-seismic regions with high heat flow value.

on average by Pamukçu *et al*. (2007) and ranging between 12 and 17 km by Oruç *et al*. (2017).

Fig. 11a shows that the earthquakes, whose focal depths are from the surface to 10 km depth, are located along the main faults, particularly at NAFZ, EAFZ, and at the western part of BZSZ (close to EAFZ) and intensely at the SE part of Lake Van. In Fig. 11b, the intensity of the earthquakes, whose focal depths range from 10 to 20 km depths, increases along NAFZ and EAFZ and particularly, in the region where NAFZ and EAFZ are close to each other, at the western part of BZSZ and

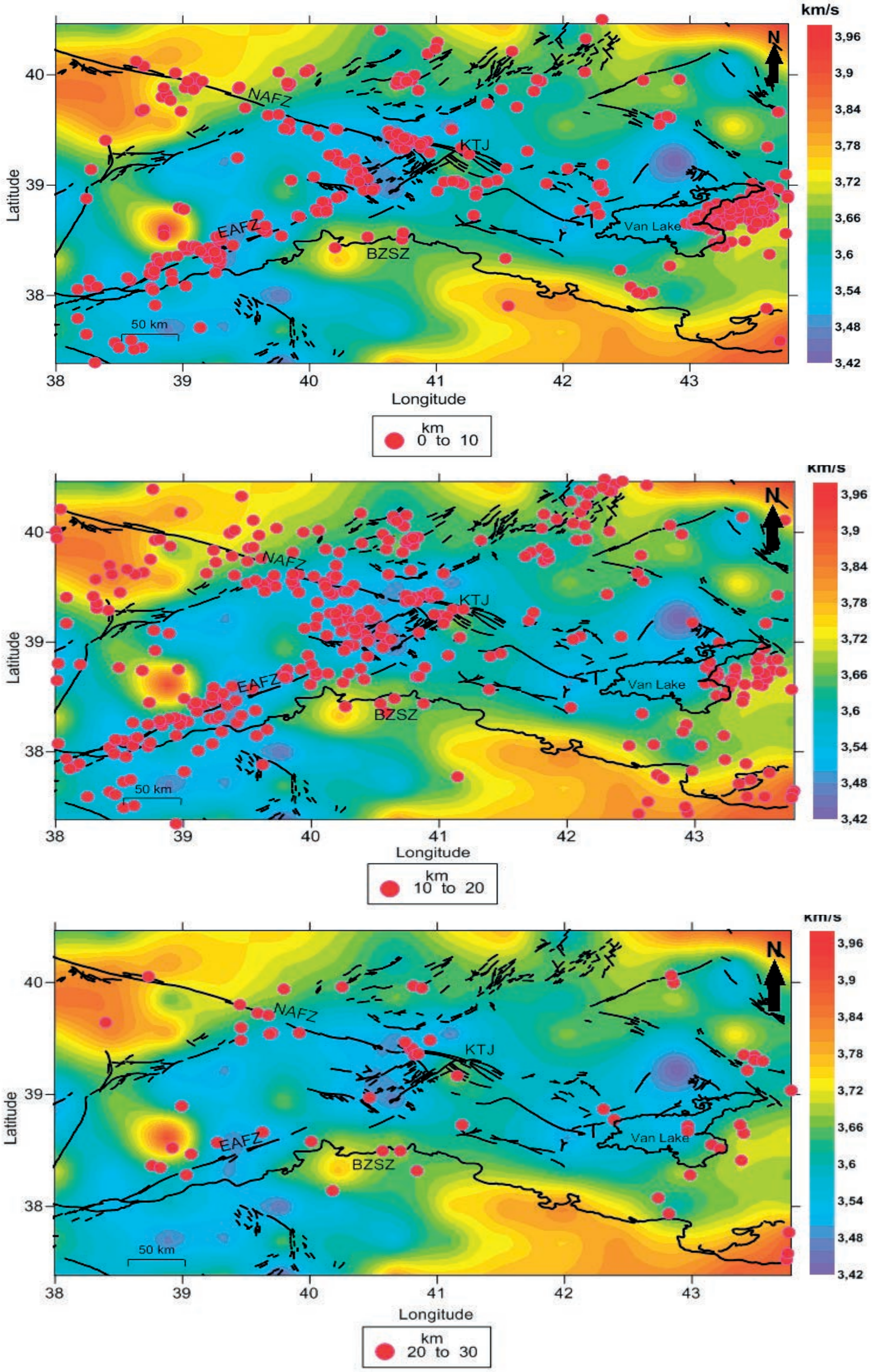

Fig. 11 - Epicentres of earthquakes (M≥2.5) between 1973 and 2016 on the V_s map estimated from V_p using A_0 = 1.5 μWm^{-3} according to different focal depth ranges: a) 0 to 10 km; b) 10 to 20 km; c) 20 to 30 km; d) 30 to 40 km; e) 40 to 50 km.

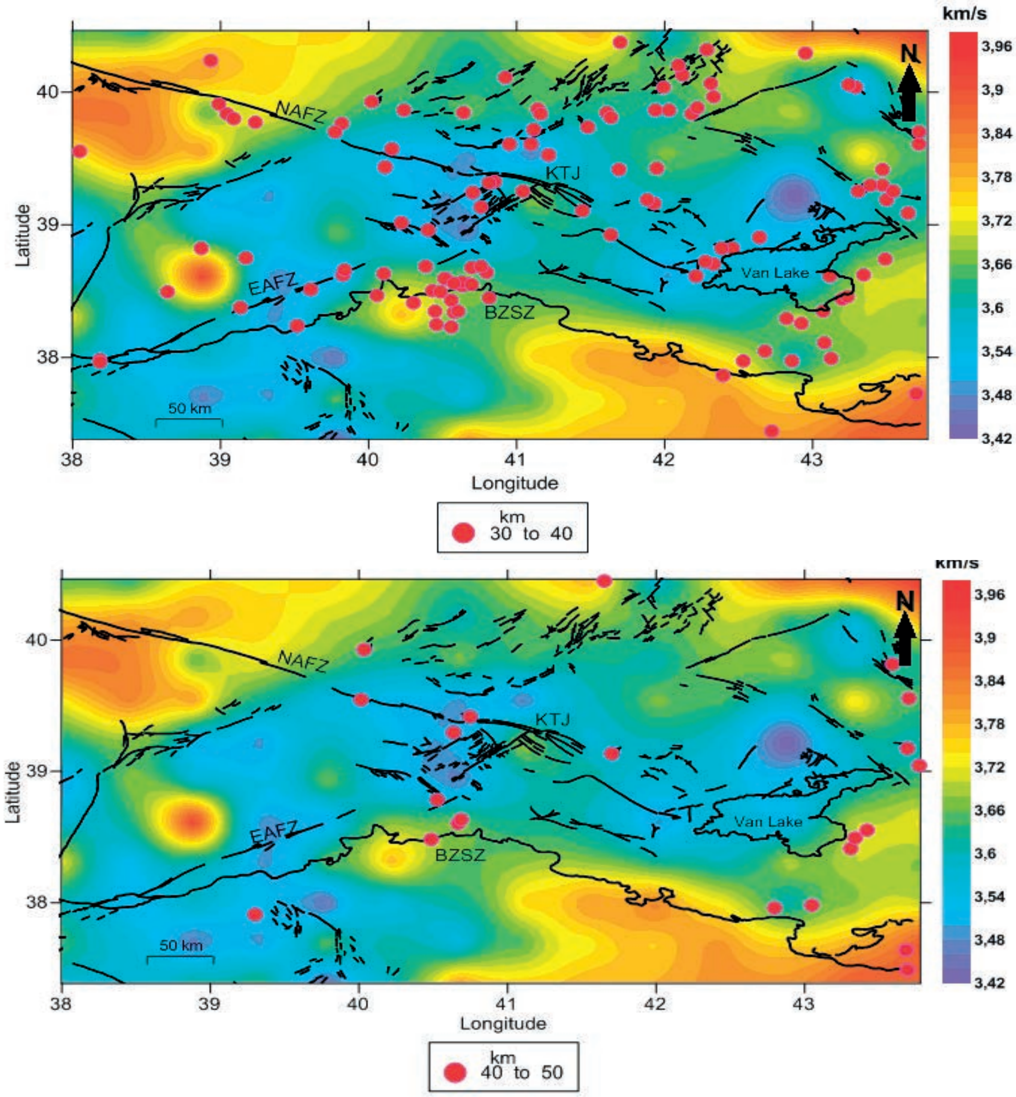

Fig. 11 - continued.

decreases at the SE part of Lake Van relative to the focal depth 0-10 km (Fig. 11a). In Figs. 11c and 11d, indicating the focal depth between 20 to 30 km and between 30 to 40 km, respectively, it can be seen that the intensity of the earthquakes decreases rapidly after 20 km depth (Fig. 11c) and increases very little after 30 km depth (Fig. 11d). The focal depth distribution, between 40 and 50 km (Fig. 11e) shows that seismicity is almost absent and it can be said that ductile feature is dominant at these depths.

According to the results of Pamukçu *et al*. (2007), based on the Euler deconvolution method, it was highlighted that the crustal features of the western and eastern parts of the region were different from each other if 41° longitude was assumed as the border. If Figs. 10 and 11 are evaluated together, due to the diversity of the heat flow, V_s values and the focal depth distributions at the western and eastern side of the region (if 41° longitude is assumed as the border), we may infer that these regions represent different crustal features as pointed out in the study by Pamukçu *et al*. (2007).

The regions along EAFZ, surrounding KTJ, and the eastern part of NAFZ include high seismicity, high heat flow and represent lower V_s values ranging between 3.42 and 3.58 km/s (Figs. 11a and 11b). The existence of high seismicity, high heat flow values and the low V_s values in these regions (Figs. 11a and 11b) verify that a lateral brittle-ductile transition and brittle features may be dominant in the crust. It may be inferred, therefore, that the origin of the heat is mantle-sourced and due to the long time-scaled friction (Bird *et al.*, 1975; Pamukçu *et al.*, 2014) between Anatolian and Arabian Plates at these regions. The asthenospheric uplifts and the frictional heating can increase the potential of the geothermal sources along EAFZ and surrounding KTJ.

5. Conclusions

In this study, the thermal conductivity, the heat flow, the heat production, and the seismic velocities (V_p and V_s) values are obtained by using calculated CPD values (Fig. 3) of eastern Anatolia. The thermal gradient values of the eastern Anatolia vary between 20 and 100 ºC/km (Fig. 4). The heat flow values are estimated for three thermal conductivity values, which are assumed as 2.5 and 2.7 $Wm^{-1}K^{-1}$ and the values vary between 50-250 (Fig. 5a) and 50-265 mW/m^2 (Fig. 5b), respectively. The heat production values are calculated for different near-surface radiogenic heat production rate coefficient (A_0) given as 1.5, 3.0 and 4.0 μWm^{-3} and are found to range between 0.10-0.85 (Fig. 6a), 0.20-1.60 (Fig. 6b) and 0.20-2.30 $\mu W/m^3$ (Fig. 6c). V_p are estimated for each heat production value obtained by different A_0 values and vary between 5.90-6.90 (Fig. 7a), 5.60-6.60 (Fig. 7b) and 5.45-6.45 km/s (Fig. 7c). For the first time, V_s are calculated for eastern Anatolia indirectly by using CPD values; V_s vary between 3.42-3.96 (Fig. 8a), 3.22-3.76 (Fig. 8b) and 3.14-3.68 km/s (Fig. 8c). The V_s values which are estimated indirectly from V_p using the heat production values estimated for A_0= 1.5 μWm^{-3} (Fig. 8a) are found to be consistent with the V_s values obtained from receiver function by Zor *et al*. (2003). If the calculated V_s values, by using A_0= 1.5 μWm^{-3} (Fig. 8a), A_0= 3 μWm^{-3} (Fig. 8b) and A_0= 4 μWm^{-3} (Fig. 8c), are evaluated, it can be seen that while the A_0 value decreases, the calculated V_s values come close to V_s values at Moho depth. The high thermal gradient, heat flow, heat production values and low seismic velocities are seen along EAFZ, surrounding KTJ and Lake Van, where there are volcanic features. Additionally, the focal depth distributions are investigated with heat flows and V_s values (Figs. 10 and 11). In Figs. 10, 11a and 11b, it can be observed how a great number of earthquakes occurred in the first 20 km depth. Therefore, it may be deduced that the rigid part of the crust for eastern Anatolia is between 10 and 20 km depth and if the 41º longitude is assumed as a border, the eastern and western sides of eastern Anatolia include different crustal features.

References

Al-Lazki A., Seber D., Sandvol E., Türkelli N., Mohamad R. and Barazangi M.; 2003: *Tomographic Pn velocity and anisotropy structure beneath the Anatolian Plateau (eastern Turkey) and the surrounding regions*. Geophys. Res. Lett., **30**, 8043, doi:10.1029/2003GL017391.

Artemieva I.M. and Money W.D.; 2001: *Thermal thickness and evolution of Precambrian lithosphere*. J. Geophys. Res., **106**, 16387-16414.

Ateş A., Bilim F. and Buyuksarac A.; 2005: *Curie Point depth investigation of central Anatolia, Turkey.* Pure Appl. Geophys., **162**, 357-371.

Aydin I., Karat H.I and Kocak A.; 2005: *Curie Point depth map of Turkey.* Geophys. J. Int., **162**, 633-640.

Bektas O.; 2013: *Thermal structure of the crust in inner east Anatolia from aeromagnetic and gravity data.* Phys. Earth Planet. Inter., **221**, 27-37.

Bektaş O., Ravat D., Buyuksarac A., Bilim F. and Ates A.; 2007: *Regional geothermal characterization of east Anatolia from aeromagnetic, heat flow and gravity data*. Pure Appl. Geophys., **164**, 975-998.

Bhattacharrya B.K. and Morley L.W.; 1965: *The delination of deep crustal magnetic bodies from total aeromagnetic anomalies*. J. Geomag. Geoelec., **17**, 237-252.

Bilim F.; 2007: *Investigation into the tectonic lineaments and thermal structure of Kutahya-Denizli Region western Anatolia, from using aeromagnetic, gravity and seismological data*. Phys. Earth Planet. Inter., **165**, 135-146.

Bilim F.; 2011: *Investigation of the Galatian volcanic complex in the northern central Turkey using potential field data*. Phys. Earth Planet. Inter., **185**, 36-43.

Bilim F., Akay T., Aydemir A. and Kosaroglu S.; 2016: *Curie Point depth, heat-flow and radiogenic heat production deduced from the spectral analysis of the aeromagnetic data for geothermal investigation on the Menderes Massif and the Aegean Region, western Turkey*. Geothermics, **60**, 44-57.

Bird P., Toksöz M.N. and Sleep N.H.; 1975: *Thermal and mechanical models of continent-continent convergence zones*. J. Geophys. Res., **80**, 4405-4416.

Bozkurt E.; 2001: *Neotectonics of Turkey - a synthesis*. Geodinamica Acta, **14**, 3-30.

Burke K. and Şengör C.; 1986: *Tectonic escape in the evolution of the continental crust*. In: Reflection seismology, The continental crust, American Geophysical Union, Washington, DC, USA, Vol. 14, pp. 41-53.

Christensen N.I.; 1996: *Poisson's ratio and crustal seismology*. J. Geophys. Res., **101,** 3139-3156.

Correia A. and Ramalho E.C.; 1999: *One-dimensional thermal models constrained by seismic velocities and surface radiogenic heat production for two main geotectonic units in southern Portugal.* Tectonophys., **306**, 261-268.

Dewey J.F., Hempton M.R., Kidd W.S.F., Saroglu F. and Sengör A.M.C.; 1986: *Shortening of continental lithospere: the neotectonics of eastern Anatolia - a young collision zone.* In: Coward M.O. and Ries A.C. (eds), Collisional Tectonics, Geol. Soc. London, Special Publ., 19, pp. 3-36.

Dolmaz M.N., Hisarli Z.M., Ustaomer T. and Orbay N.; 2005: *Curie Point depths based on spectrum analysis of aeromagnetic data, west Anatolian extensional province, Turkey*. Pure Appl. Geophys., **162**, 571-590.

Durrance E.M.; 1986: *Radioactivity in geology: principles and applications*. Ellis Horwood Ltd, Chichester, England, 441 pp.

Gök R., Sandvol E., Türkelli N., Seber D. and Barazangi M.; 2003: *Sn attenuation in the Anatolian and Iranian Plateau and surrounding regions*. Geophys. Res. Lett., **30**, doi:10.1029/2003GL018020.

Gök R., Pasyanos M. and Zor E.; 2007: *Lithospheric structure of the continent-continent collision zone: eastern Turkey.* Geophys. J. Int., **169**, 1079-1088.

Gürbüz C., Türkelli N., Bekler T., Gök R., Sandvol E., Seber D. and Barazangi M.; 2004: *Seismic event location calibration using the eastern Turkey broadband seismic network: analysis of the Agri dam explosion.* Bull. Seismol. Soc. Am., **94**, 1166-1171.

Jaupart C.; 1986: *On the average amount and vertical distribution of radioactivity in the continental crust.* In: Burrus J. (ed), Thermal modeling in sedimentary basins, Editions Technip, Paris, France, pp. 33-47.

Keskin M.; 2003: *Magma generation by slab steepening and breakoff beneath a subduction-accretion complex: an alternative model for collision-related volcanism in eastern Anatolia, Turkey.* Geophys. Res. Lett., **30**, 8046.

Koçyiğit A., Yilmaz A., Adamia S. and Kuloshvili S.; 2001: *Neotectonics of east Anatolian Plateau (Turkey) and Lesser Caucasus: implication for transition from thrusting to strike-slip faulting.* Geodinamica Acta, **14**, 177-195.

Lachenbruch A.H.; 1968: *Preliminary geothermal model of the Sierra Nevada*. J. Geophys. Res., **73**, 6977-6989.

Lachenbruch A.H.; 1970: *Crustal temperature and heat production: implication of the linear heat flow relationship.* J. Geophys. Res., **75**, 3291-3300.

McKenzie D.; 1972: *Active tectonics of the Mediterranean Region*. Geophys. J. Int., **30**, 109-185.

MTA; 2005: *The General Directorate of Mineral Research and Exploration of Turkey, Aeromagnetic Data*

Obande G.E., Lawal K.M. and Ahmed L.A.; 2014: *Spectral analysis of aeromagnetic data for geothermal investigation of Wikki Warm Spring, north-east Nigeria*. Geothermics, **50**, 85-90.

Okubo Y., Graf J.R., Hansen R.O., Ogawa K. and Tsu H.; 1985: *Curie Point depths of the Island of Kyushu and surrounding areas, Japan*. Geophys., **53**, 481-494.

Oruç B., Gomez-Ortiz D. and Petit C.; 2017: *Lithospheric flexural strength and effective elastic thicknesses of the eastern Anatolia (Turkey) and surrounding region*. J. Asian Earth Sci., **150**, 1-13.

Özaçar A.A., Gilbert H. and Zandt G.; 2008: *Upper mantle discontinuity structure beneath east Anatolian Plateau (Turkey) from receiver functions*. Earth Planet. Sci. Lett., **269**, 427-435.

Pamukçu O.A. and Akçığ Z.; 2011: *Isostasy of the eastern Anatolia (Turkey) and discontinuities of its crust.* Pure Appl. Geophys., **168**, 901-917.

Pamukçu O.A., Akçığ Z., Demirbaş S. and Zor E.; 2007: *Investigation of crustal thickness in eastern Anatolia using gravity, magnetic and topographic data.* Pure Appl. Geophys., **164**, 2345-2358.

Pamukçu O., Akçığ Z., Hisarli M. and Tosun S.; 2014: *Curie Point depths and heat flow of eastern Anatolia (Turkey).* Energy Sources Part A, **36**, 2699-2706.

Pamukçu O., Gönenç T., Çırmık A.Y., Demirbaş Ş. and Tosun S.; 2015: *Vertical and horizontal analysis of crustal structure in eastern Anatolia Region.* Bull. Miner. Res. Explor., **151**, 217-229.

Pearce J.A., Bender J.F., DeLong S.E., Kidd W.S.F., Low P.J., Guner Y., Sarolu F., Yilmaz Y., Moorbath S. and Mitchel J.G.; 1990: *Genesis of collision volcanism in eastern Anatolia, Turkey*. J. Volcanol. Geotherm. Res., **44**, 189-229.

Pollack H.N. and Chapman D.S.; 1977: *On the regional variation of heat flow, geotherms, and lithospheric thickness.* Tectonophys., **38**, 279-296.

Rotstein Y. and Kafka A.L.; 1982: *Seismotectonics of the southern boundary of Anatolia, eastern Mediterranean Region: subduction, collision, and arc jumping.* J. Geophys. Res., **87**, 7694-7706.

Rybach L.; 1978/1979: *The relationship between seismic velocity and radioactive heat production in crustal rocks: an exponential law.* Pure Appl. Geophys., **117**, 75-82.

Rybach L. and Buntebarth G.; 1982: *Relationship between the petrophysical properties density, seismic velocity, heat generation and mineralogical constitution*. Earth Planet. Sci. Lett., **57**, 367-376.

Rybach L. and Buntebarth G.; 1984: *The variation of heat generation, density and seismic velocity with rock type in the continental crust.* Tectonophys., **103**, 309-344.

Saleh S., Salk M. and Pamukcu O.; 2013: *Estimating Curie depth and heat flow map for northern Red Sea Rift of Egypt and its surroundings, from aeromagnetic data.* Pure Appl. Geophys., **170**, 863-885.

Sandvol E., Türkelli N., Zor E., Gök R., Bekler T., Gürbüz C., Seber. D. and Barazangi M.; 2003: *Shear wave splitting in a young continent - continent collision: an example from eastern Turkey*. Geophys. Res. Lett., **30**, 8041, doi:10.1029/2003GL017390.

Şengör A.M.C., Özeren S., Genç T. and Zor E.; 2003: *East Anatolian high plateau as a mantle-supported, north-south shortened domal structure.* Geophys. Res. Lett., **30**, 8045, doi:10.1029/2003GL017858.

Spector A. and Grant F.S.; 1970: *Statistical models for interpretation aeromagnetic data*. Geophys., **35**, 293-302.

Springer M.; 1999: *Interpretation of heat-flow density in the central Andes*. Tectonophys., **306**, 377-395.

Tanaka A., Okubo Y. and Matsubayashi O.; 1999: *Curie Point depth based on spectrum analysis of the magnetic anomaly data in east and southeast Asia*. Tectonophys., **306**, 461-470.

Tsokas G.N., Hansen R.O. and Fytikas M.; 1998: *Curie Point depth of the island of Crete (Greece).* Pure Appl. Geophys., **152**, 747-757.

Turcotte D.L. and Schubert G.; 1982: *Geodynamics: applications of continuum physics to geological problems.* John Wiley, New York, USA, 450 pp.

Türkelli N., Sandvol E., Zor E., Gök R., Bekler T., Al-Lazki A., Karabulut H., Kuleli S., Eken T., Gurbuz C., Bayraktutan S., Seber D. and Barazangi M.; 2003: *Seismogenic zones in eastern Turkey.* Geophys. Res. Lett., **30**, 8039, doi:10.1029/2003GL018023.

Uyanik N.A. and Akkurt I.; 2010: *Determination of natural radioactivity in Isparta - Çünür Hill covered with alkaline volcanics*. Afyon Kocatepe Univ. J. Sci., **9**, 35-42.

Uyanik N.A., Akkurt I. and Uyanik O.; 2010: *A ground radiometric study of uranium, thorium and potassium in Isparta, Turkey.* Ann. Geophys., **53**, 25-30.

Uyanik N.A., Öncü Z., Uyanik O., Bozcu M., Akkurt I., Günoglu K. and Yagmurlu F.; 2015: *Distribution of natural radioactivity from 40K radioelement in volcanics of Sandıklı - Suhut (Afyon) Area.* Acta Phys. Pol., **128**, B438-440, doi:10.12693/APhysPolA.128.B-438.

Watts A.B.; 2001: *Isostasy and flexure of the Lithosphere.* Cambridge University Press, Cambridge, England, pp. 87-283.

Zor E., Sandvol E., Gürbüz C., Türkelli N., Şeber D. and Barazangi M.; 2003*: The crustal structure of the east Anatolian Plateau (Turkey) from receiver functions.* Geophys. Res. Lett., **30**, 8044.

Corresponding author: Ayça Cırmık
Department of Geophysical Engineering, Engineering Faculty, Dokuz Eylul University
Tınaztepe Campus, Buca, TR–35160 Izmir, Turkey
Phone: +90 2323017282; e-mail: ayca.yurdakul@deu.edu.tr